PASSIVE EARTH PRESSURES: THEORIES AND TESTS

By J. Michael Duncan,[1] Honorary Member, ASCE, and Robert L. Mokwa,[2] Member, ASCE

ABSTRACT: The magnitude of the passive earth pressure that resists the movement of a structure is controlled by the amount the structure moves and the direction in which it moves, strength and stiffness of the soil that resists its movement, friction or adhesion on the interface between the structure and soil, and shape of the structure. The Log Spiral Theory, corrected for 3D effects, provides an accurate means of computing ultimate passive pressures. A hyperbolic expression, together with estimated values of soil modulus and ultimate resistance, provides a means of estimating the relationship between structural movement and passive resistance. It is essential that the soil strength and stiffness used in making these estimates should be appropriate for the soil and the drainage conditions involved. The results of an undrained passive pressure load test in stiff sandy silt and a drained passive pressure load test in well-graded gravel are compared with passive pressures computed using the methods discussed. Reasonable agreement between the calculated and measured values shows that the Log Spiral Theory, corrected for 3D effects, and the hyperbolic load-deflection relationship provide an adequate means of estimating passive resistance for a wide range of conditions.

INTRODUCTION

Passive earth pressures play an important role in soil-structure interaction. As shown in Fig. 1, they resist lateral movement of structures and provide stabilizing forces for anchor blocks, retaining walls, and laterally loaded pile caps.

Passive pressures induce large loads in integral bridges. When rising temperatures cause an integral bridge to expand in length, pushing its abutments against the approach fills, passive resistance applies a compressive load to the bridge through the abutments. The superstructure must be designed to resist these loads.

Maximum passive pressures can be computed using the well-known Rankine, Coulomb, and Log Spiral earth pressure theories. However, each of these theories has limitations and none provides information on the relationship between resistance and movement.

In the following sections, the factors that control the magnitudes of passive earth pressures are reviewed and the strengths and weaknesses of the various methods of computing passive earth pressures are discussed. A numerical procedure for applying the Log Spiral earth pressure theory is described, and a rational method for computing the relationship between resistance and movement is explained. Computed results are compared with passive forces measured in field tests.

FACTORS THAT CONTROL PASSIVE EARTH PRESSURES

The passive resistance that develops when a structure moves against soil depends on (1) the amount and direction of the movement; (2) strength and stiffness of the soil; (3) friction and/or adhesion between the structure and soil; and (4) shape of the structure. Each of these factors has an important influence on the magnitude of passive earth pressure.

Movement of Structure

In the case shown in Fig. 2, the structure moves horizontally while the soil moves both horizontally and upward. As a result of the upward movement of the soil with respect to the structure, there is an upward shear force on the structure and a downward shear force on the soil. Therefore the resultant passive earth pressure force E_p acts at an angle to the soil-structure boundary. The condition shown in Fig. 2 is representative of situations where the structure is massive or supported on piles and the upward component of the passive resistance is insufficient to cause upward movement of the structure.

In other circumstances, which are illustrated in Fig. 3, the upward component of the passive resistance is large enough to cause upward movement of the structure, and the soil and structure move together. This will be the case for structures such as anchor blocks, which are relatively light and are not supported on piles.

Soil Strength and Stiffness

Both soil strength and soil stiffness are important in determining the amount of passive resistance that develops in a given circumstance. The greater the strength of the soil, the larger is the maximum possible passive pressure. The stiffer the soil, the greater is the passive pressure induced by a given amount of movement. To evaluate passive resistance over a range of movements or to determine whether or not the maximum possible passive resistance will be developed by a given amount of movement, both soil strength and soil stiffness must be considered.

For conditions where the soil has low permeability and loads are quickly applied, passive resistance is governed by the undrained strength of the soil. Drained strength controls passive resistance under short-term conditions if the permeability of the soil is high, and under long-term conditions in all soils. Both cohesion and friction contribute to passive resistance.

Interface Friction and Adhesion

As noted above, relative shear displacements between soil and structure result in passive resistance that is inclined at an angle δ to the normal to the interface, as shown in Figs. 2 and 3. The magnitude of δ is governed by three factors:

- The maximum possible value of δ depends on the roughness of the interface and the properties of the soil. It is convenient to characterize values of δ_{max} in terms of the ratio δ_{max}/ϕ, where ϕ is the angle of internal friction of the soil. Potyondy (1961) conducted interface shear tests on a variety of structural materials and soils. The values of δ_{max}/ϕ listed in Table 1, which are the smallest found by Potyondy, provide conservative estimates of δ_{max}/δ.

[1]Univ. Distinguished Prof., Dept. of Civ. and Envir. Engrg., Virginia Polytechnic Inst., Blacksburg, VA 24061-0105. E-mail: jmd@vt.edu.

[2]Sr. Geotechnical Engr., Terracon, 11849 W. Executive Dr., Boise, ID 83713.

Note. Discussion open until August 1, 2001. To extend the closing date one month, a written request must be filed with the ASCE Manager of Journals. The manuscript for this paper was submitted for review and possible publication on January 7, 2000; revised October 6, 2000. This paper is part of the ***Journal of Geotechnical and Geoenvironmental Engineering***, Vol. 127, No. 3, March, 2001. ©ASCE, ISSN 1090-0241/01/0003-0248–0257/$8.00 + $.50 per page. Paper No. 22226.

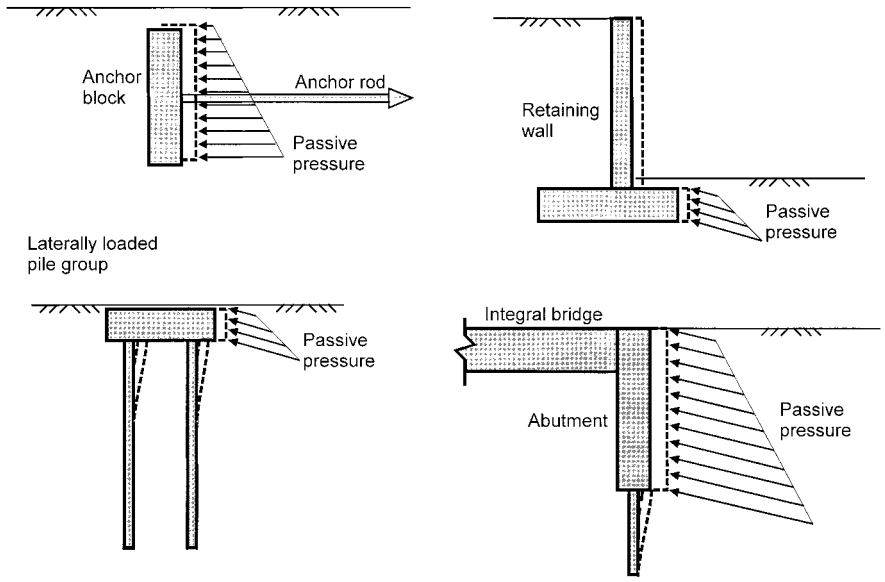

FIG. 1. Examples of Conditions Where Passive Pressures Resist Displacements of Structures

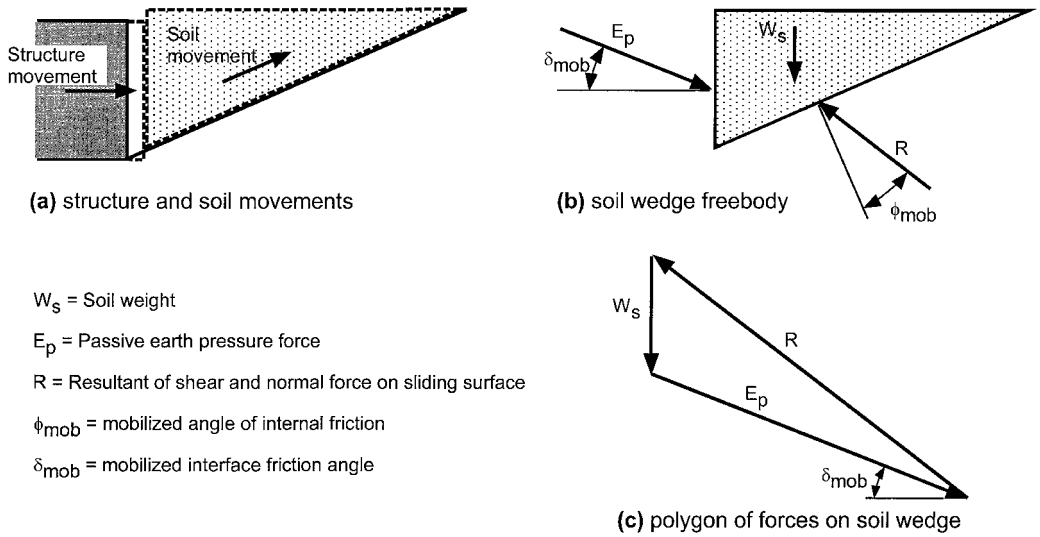

FIG. 2. Movements, Forces, and Equilibrium Requirements for Passive Pressure Conditions

- Some amount of relative shear displacement across the interface is required to mobilize interface friction. The amount of relative shear displacement required to mobilize the full strength of the interface is not large, typically no more than 0.1–0.25 in. (2.5–6 mm). Smaller relative displacements across the interface will result in only partial mobilization of the interface friction. Therefore δ_{mob} will be less than or equal to δ_{max}:

$$\delta_{mob} \leq \delta_{max} \tag{1}$$

- In conditions such as the one shown in Fig. 3, the value of δ_{mob} is controlled by the requirements of vertical equilibrium. As shown in Fig. 3(c), vertical equilibrium of the relatively light-weight anchor block requires that the following relationship must be satisfied:

$$\delta_{mob} \leq \arctan\left(\frac{W_{ab}}{T}\right) \tag{2}$$

where δ_{mob} = mobilized friction angle; W_{ab} = weight of anchor block; and T = tie-rod force (the horizontal force exerted on the anchor block). Thus equilibrium requirements may impose a third condition on δ_{mob}, in addition to the strength of the interface and the amount of relative shear displacement.

The limitation on the value of δ_{mob} caused by the weight of the structure applies mainly to relatively light structures such as anchor blocks, where the weight of the structure is smaller than the maximum possible vertical component of the passive pressure force. If the weight of the structure is greater than the vertical component of the passive pressure force, slip will occur on the interface between the structure and soil and the value of δ will be controlled by the properties of the interface. This would be the case, for example, in most retaining walls where the passive resistance against a buried toe is small compared to the weight of the wall or for a pile cap or integral bridge abutment that is restrained vertically by the piles that support it.

Cohesive soils may adhere to structures, resulting in additional shear stresses on the soil-structure interface. The maximum possible value of adhesion c_a is equal to the cohesion of the soil c. The adhesion can be characterized conveniently in terms of $\alpha = c_a/c$, which varies from about 0.5 for stiff soils to about 0.9 for soft soils.

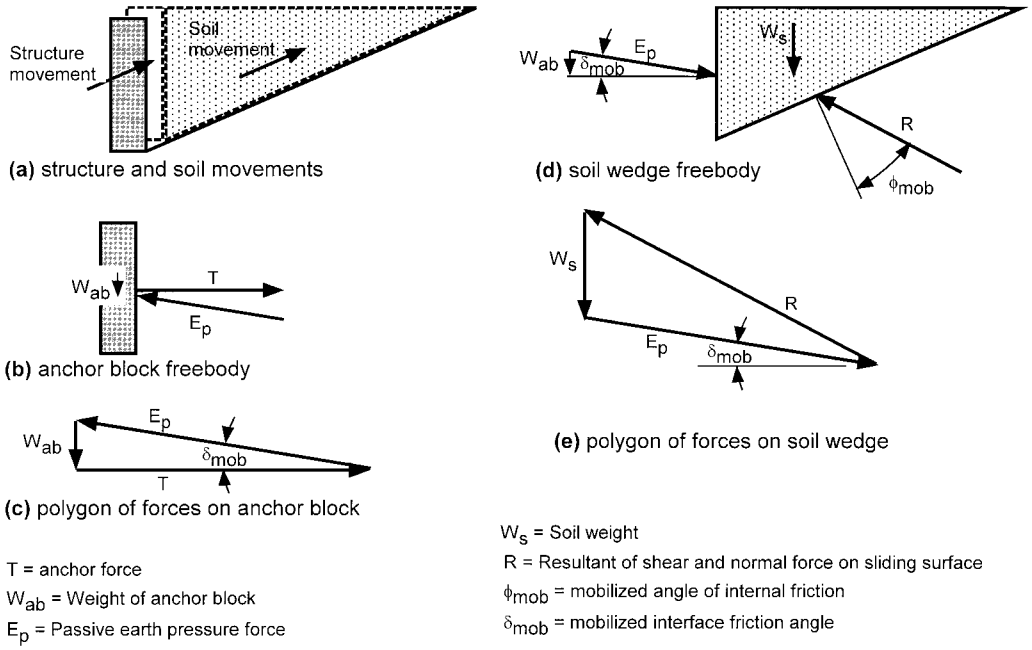

FIG. 3. Condition Where Mobilized Interface Friction Angle Is Controlled by Equilibrium Requirements

TABLE 1. Minimum Values of δ_{max}/ϕ Determined by Potyondy (1961)

Soil type (1)	Structural Material		
	Steel (δ_{max}/ϕ) (2)	Concrete (δ_{max}/ϕ) (3)	Wood (δ_{max}/ϕ) (4)
Sand	0.54	0.76	0.76
Silt and clay	0.54	0.50	0.55

Note: δ_{max} = interface friction angle, ϕ = angle of internal friction of soil.

Structure Shape

Conventional earth pressure theories are based on 2D analyses of a cross section through structure and soil. It is assumed implicitly that the conditions at all cross sections along the length of a structure are the same, ignoring the influence of the different conditions at the ends of the structure. The boundary conditions at the ends of a structure are quite different from those at the center. These differences between conditions at the center and at the ends can have a significant influence on passive resistance, especially for short structures. Ovesen (1964) conducted an extensive series of passive pressure model tests to investigate this effect. His tests showed that passive earth pressures against short structures are higher than those predicted by conventional theory and the difference can be quite significant.

Brinch Hansen (1966) developed a method for correcting the results of conventional passive pressure theories for shape (or 3D) effects, based on Ovesen's test results. His method is shown in Fig. 4. For the example shown in Fig. 4, the passive resistance is twice as high as that computed from conventional theory as a result of the 3D effects. Consequently, the shape of the structure is an important factor that should be included in analyses of passive resistance.

PASSIVE EARTH PRESSURE THEORIES

Two earth pressure theories are widely used in geotechnical engineering. They are the Coulomb Theory (Coulomb 1776), which treats the passive pressure problem in terms of forces, and the Rankine Theory (Rankine 1857), which treats the problem in terms of stresses. Both theories are well known and are described in nearly every soil mechanics textbook.

The logarithmic spiral earth pressure theory is less widely used than the Rankine and Coulomb theories because of its complexity, but it provides more accurate estimates of passive pressures for conditions where the interface friction angle δ is more than about 40% of the angle of internal friction ϕ. The theory has been described in detail in Terzaghi (1943) and Terzaghi et al. (1996).

A number of investigators have developed alternative theoretical procedures for evaluating K_p, and these different approaches generally confirm the accuracy of the Log Spiral Theory for a wide range of values of δ and ϕ. Chen and Su (1994), Kumar and Subga Rao (1997), Subra (2000), and Zhu and Quian (2000) computed values of K_p by means of numerical analyses based on plasticity theory. All found close agreement with the Log Spiral Theory. Similarly, Martin and Nad Yun (1995), who used FLAC numerical analyses to evaluate passive pressures on bridge abutments, found fairly close agreement with the Log Spiral Theory for large values of the wall friction angle δ. Only Shields and Tolumay (1973), who assumed that ''all the vertical shear forces are lost close to the wall,'' found theoretical results much different from those of the Log Spiral Theory. Shields and Tolumay justified their assumption on the basis that it resulted in lower values of K_p than the more theoretically consistent Log Spiral Theory, which is generally agreed to be the most accurate theory for passive pressures.

The Rankine, Coulomb, and Log Spiral theories all have advantages and limitations, which are summarized in Table 2. The main disadvantage of the Coulomb Theory stems from the fact that it is assumed that the passive pressure failure mechanism involves sliding along a plane surface. As a result, values of K_p computed using the Coulomb Theory are too high when the value of δ is larger than about 0.4ϕ. As the value of δ approaches ϕ, the error in the Coulomb value of K_p becomes very large, as shown in Table 3. For values of $\delta < 0.4\phi$, however, the Coulomb Theory is an accurate method of evaluating passive pressures.

The Log Spiral Theory uses the curved failure surface shown in Fig. 5, which represents a more probable failure mechanism for values of $\delta > 0.4\phi$ and results in smaller values of K_p for this range of δ than does the Coulomb Theory. Be-

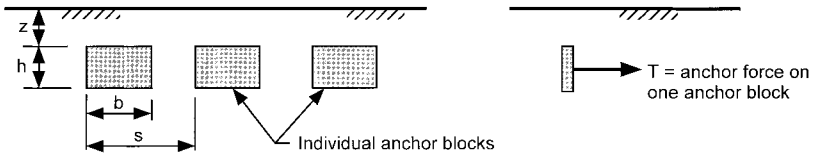

$T_{ult} = (M)\ (K_p - K_a)\ (p_o')\ (b)\ (h)$

M = correction factor to account for 3D effects on passive resistance (Ovesen, 1964)

$$M = 1 + (K_p - K_a)^{0.67}\left[1.1E^4 + \frac{1.6\ B}{1 + 5\ (b/h)} + \frac{0.4(K_p - K_a)\ E^3\ B^2}{1 + 0.05\ (b/h)}\right]$$

K_p = coefficient of passive earth pressure

K_a = coefficient of active earth pressure

$B = 1 - (b/s)^2$

$E = 1 - h/(z+h)$

p_o' = effective overburden pressure at midheight of anchor block

Example: h = 2 ft, b = 2 ft, z = 2 ft, s = 8 ft, ϕ' = 35 degrees, γ = 120 pcf, and $\delta = 0$

B = 0.94, E = 0.5, Kp - Ka = 3.42, M = 2.04, p_o' = 360 psf

$T_{ult} = (2.04)(3.42)(360)(2)(2) = 10{,}000$ lb

FIG. 4. Ovesen-Brinch Hansen Method of Correcting for 3D Effects in Passive Earth Pressures [after Ovensen (1964) and Brinch Hansen (1966)]

TABLE 2. Advantages and Limitations of Passive Earth Pressure Theories

Theory (1)	Advantages (2)	Limitations (3)
Rankine	Simplest method	It is assumed that $\delta = i$, where i = inclination of ground surface; applies only to simple conditions (planar ground surface, uniform surcharge, homogeneous soil)
Coulomb	Applicable for any value of wall friction $0 \leq \delta \leq \phi$; easy to apply through charts, tables, or formulas; can account for more complex conditions (irregular ground surface, nonuniform surcharge, nomhomogeneous soil conditions) through graphical analyses	Passive pressures are too high for values of $\delta > 0.4\phi$; complex conditions require graphical analyses
Log spiral charts and tables	Accurate for any value of δ; easy to apply	Applicable only to simple conditions; does not accommodate cohesive component of shear strength
Log spiral graphical solution	Accurate for any value of δ; can accommodate cohesive as well as frictional soil strength; is applicable to complex conditions	Requires complex graphical analyses
Log spiral numerical solution	Accurate for any value of δ; can accommodate cohesive as well as frictional strength; with Ovesen's correction, accounts for 3D effects	Computer program such as PYCAP is needed; PYCAP is only applicable to simple conditions (level ground, vertical wall, uniform surcharge, and homogeneous soil)

TABLE 3. Comparison of K_p Values Computed by Rankine, Coulomb, and Log Spiral Theories for Level Ground Surface and $\phi = 40°$

Wall friction (δ/ϕ) (1)	Rankine Theory (K_p) (2)	Coulomb Theory (K_p) (3)	Log Spiral Theory (K_p) (4)
0	4.6	4.6	4.6
0.2	NA	6.3	6.6
0.4	NA	9.4	9.0
0.6	NA	15.3	11.9
0.8	NA	30.4	15.5
1.0	NA	92.6	17.5

Note: NA = not applicable.

cause both Coulomb and Log Spiral are upper-bound theories, the smaller the value of K_p, the more accurate it is. Thus the Log Spiral Theory is superior to the Coulomb Theory for conditions where δ exceeds 0.4ϕ.

The Log Spiral Theory can be employed in three ways. The simplest is to use tables or charts of passive pressure coefficients based on the Log Spiral Theory, which are found in Caquot and Kerisel (1948) and NAVFAC (1982). The limitations of these charts and tables are that they apply only to simple conditions and do not provide a means of accommodating the cohesive component of shear strength. The most general method of applying the Log Spiral Theory is the graphical procedure explained in Terzaghi (1943) and Terzaghi et al. (1996). However, graphical solutions require considerable time and effort.

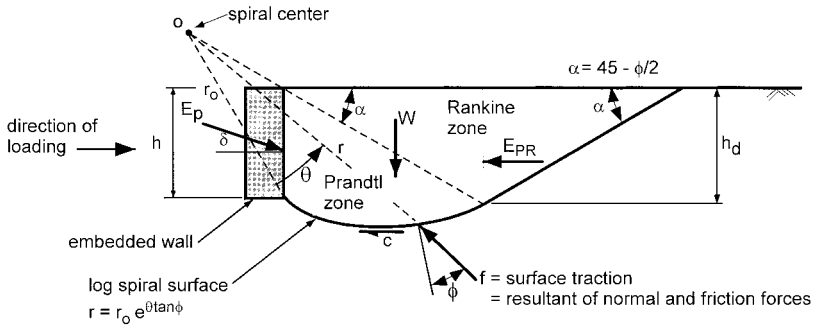

FIG. 5. Log Spiral Failure Mechanism

A third alternative for applying the Log Spiral Theory is numerical analysis. The writers have developed an Excel spreadsheet computer program called PYCAP that is based on the Log Spiral Theory and minimizes the effort required for solution. The spreadsheet is limited to vertical walls, horizontal ground surface, and uniform surcharge. In addition to the Log Spiral Theory, the spreadsheet includes the Ovesen-Brinch Hansen correction for 3D effects, making it applicable to short as well as long structures.

LOG SPIRAL NUMERICAL ANALYSES

Because graphical analyses are complex and time-consuming, a spreadsheet was developed to perform log spiral analyses numerically. The numerical method used in the spreadsheet is based on procedures similar to the graphical analysis approach described by Terzaghi (1943) and Terzaghi et al. (1996).

The failure mechanism is assumed to consist of a Prandtl zone near the wall and a Rankine zone at the ground surface, as shown in Fig. 5. The shape of the critical log spiral and the corresponding passive resistance are determined by iteration. Various positions of the center of the spiral are tried, and for each one, three components of passive resistance are computed:

- The resistance due to the weight and angle of internal friction of the soil
- The resistance due to the surcharge and the angle of internal friction of the soil
- The resistance due to the cohesion of the soil

The position of the spiral center is varied until one is found that results in the smallest total passive resistance (smallest sum of the three components), with a resolution of 1%.

It was found that numerical difficulties occurred with this method for values of interface friction angle $\delta < 2°$. For values of $\delta < 2°$, the Rankine solution is employed.

The spreadsheet computes the total passive resistance on the structure P_{ult} as well as the passive resistance per unit length of structure E_p. These measures of passive resistance are related by the following equation:

$$P_{ult} = (E_p)(M)(b) \tag{3}$$

where P_{ult} = total passive resistance on the structure (units of force); E_p = passive resistance per unit length (units of force/length); M = Ovesen-Brinch Hansen correction factor for 3D effects (dimensionless); and b = length of structure perpendicular to plane of analysis (units of length).

Ovesen's tests were performed on compacted sand with friction angles ranging from $\phi = 32°$ to 41°. The maximum value of $(K_p - K_a)$ was 5.7 in Ovesen's tests, and M did not exceed a value of about 2. As a conservative measure, an upper limit of 2.0 was placed on the value of M that is used in the spreadsheet.

It was found that numerical difficulties occurred when the angle of internal friction ϕ approached zero. For $\phi = 0$, a different method of computing passive resistance is used, which follows the sliding wedge method developed by Reese (1958). The sliding wedge method considers a 3D failure mechanism, and the Ovesen-Brinch Hansen correction is therefore not applied in this case.

LOAD-DEFLECTION BEHAVIOR

The variation of passive resistance with deflection is approximated in the spreadsheet by a hyperbolic relationship of the form

$$P = \frac{y}{\left[\frac{1}{K_{max}} + R_f \frac{y}{P_{ult}}\right]} \tag{4}$$

where P = passive resistance (units of force); P_{ult} = ultimate (maximum) passive resistance (units of force), computed as described previously; y = deflection (units of length); K_{max} = initial stiffness = initial slope of the load-deflection curve (units of force/length); and R_f = failure ratio = P_{ult}/hyperbolic asymptote (dimensionless). The form of this relationship is shown in Fig. 6.

The value of K_{max} is calculated using the elastic solution for horizontal displacements of a uniformly loaded vertical rectangular area in an elastic half-space developed by Douglas and Davis (1964). The soil is represented as an elastic medium with properties E (Young's modulus) and ν (Poisson's ratio). The deflection of the structure is taken as the average of the deflections at the corners. This procedure is somewhat approximate, because the Douglas and Davis solution considers a flexible, uniformly loaded rectangular area, whereas structures are usually rigid in comparison with the soil against which they bear. However, the approximation involved in the elastic solution is likely to be small in comparison with the uncertainties inherent in estimating values of E and ν for soil.

The failure ratio R_f is the ratio of the ultimate passive pressure load divided by the hyperbolic asymptotic value of pas-

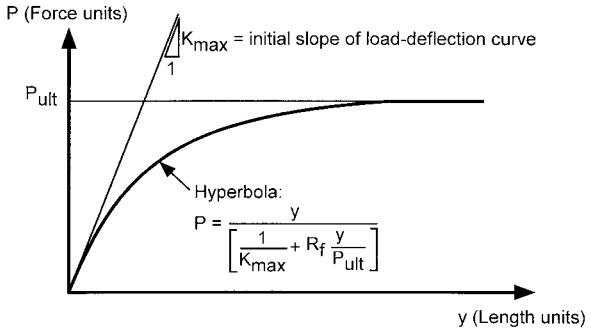

FIG. 6. Hyperbolic Load-Deflection Curve

TABLE 4. E_i Values for Soils at Shallow Depths (2–5 ft)

Sands and Gravels (based on data from D'Appolonia et al. (1970) and Duncan et al. (1980).

Density	D_r	N_{60}	Normally loaded	Preloaded or compacted
Loose	40%	3	E_i = 200 – 400 ksf	E_i = 400 – 800 ksf
Medium	60%	7	E_i = 300 - 500 ksf	E_i = 500 – 1000 ksf
Dense	80%	15	E_i = 400 - 600 ksf	E_i = 600 – 1200 ksf

E_i = initial tangent modulus 1 ksf = 47.9 kPa

D_r = relative density

N_{60} = Standard Penetration Test blow count, adjusted to 60% hammer energy

Naturally Occurring Cohesive Soils (from Duncan and Buchignain, 1976) and Lambe and Whitman (1969).

	Short-term modulus		Long-term modulus	
Plasticity Index	NC	OC	NC	OC
<30	E_i/S_u = 600 - 1200	E_i/S_u = 400 - 800	E_i/S_u = 50 - 150	E_i/S_u = 300 - 600
30 – 50	E_i/S_u = 300 - 600	E_i/S_u = 200 - 400	E_i/S_u = 30 - 100	E_i/S_u = 150 - 300
>50	E_i/S_u = 150 - 300	E_i/S_u = 100 - 200	E_i/S_u = 15 - 50	E_i/S_u = 100 - 200

NC = normally consolidated
OC = overconsolidated

S_u = undrained shear strength

Compacted Cohesive Soils (CL, RC = 95% to 100% of Standard Proctor maximum) from Duncan et al. (1980).

Compaction water content	Short-term modulus	Long-term modulus
w = opt. – 2%	E_i = 400 – 1200 ksf	E_i = 120 – 400 ksf
w = optimum	E_i = 200 – 600 ksf	E_i = 120 – 400 ksf
w = opt. + 2%	E_i = 100 – 300 ksf	E_i = 120 – 400 ksf

E_i = initial tangent modulus 1 ksf = 47.9 kPa
CL = clay of low plasticity
RC = relative compaction
opt. = optimum water content

sive resistance. There is no rational way to determine the most appropriate value of R_f unless the measured response is available, but the value of R_f can be estimated based on experience. Duncan and Chang (1970) found that values of R_f ranging from 0.75 to 0.95 were appropriate for hyperbolic representations for stress-strain curves, and the same range of values has been found to work well for fitting hyperbolic load-deflection curves to the test data discussed in the following paragraphs. A value of R_f = 0.85 was used for all the hyperbolic load-deflection curves discussed in this paper.

Because the elastic solution is used to estimate the initial slope of the load-deflection curve, it is appropriate to use initial tangent modulus values in the calculation. Undrained modulus values should be used for short-term conditions in soils with low permeability, and drained modulus values should be used for short-term conditions in soils with high permeability and for long-term conditions in all soils. In most cases laboratory tests are of little value for determining modulus values for soils, because modulus values for cohesive soils are greatly reduced by even moderate amounts of sample disturbance and it is not practical to obtain undisturbed samples of cohesionless soils. Table 4 contains correlations that can be used to estimate modulus values for soils at shallow depths, which are appropriate for passive pressure problems.

Poisson's ratio is also needed to compute K_{max}. Values of Poisson's ratio for soils can be approximated by the following empirical equation:

$$\nu = \frac{1 - \sin \phi}{2 - \sin \phi} \tag{5}$$

where ν = Poisson's ratio (dimensionless); and ϕ = angle of internal friction (degrees).

The value of ϕ should be the total stress shear strength parameter ϕ_u for short-term undrained conditions and the effective stress shear strength parameter ϕ' for long-term drained conditions.

Poisson's ratio has only a secondary influence on the value of K_{max}, and the approximations involved in (5) are unlikely to be significant.

PASSIVE PRESSURE LOAD TESTS

Passive pressure load tests were performed at the Virginia Polytechnic Institute (Virginia Tech) field test site at Kentland Farms near Blacksburg, Va. The tests were performed using the test arrangement shown in Fig. 7. Using a pile group as a reaction, horizontal loads were applied to a reinforced concrete anchor block 3.5-ft high, 6.3-ft long, and 3.0-ft thick (1.1 × 1.9 × 0.9 m). Two passive pressure tests were performed, one with the anchor block bearing against natural ground and the

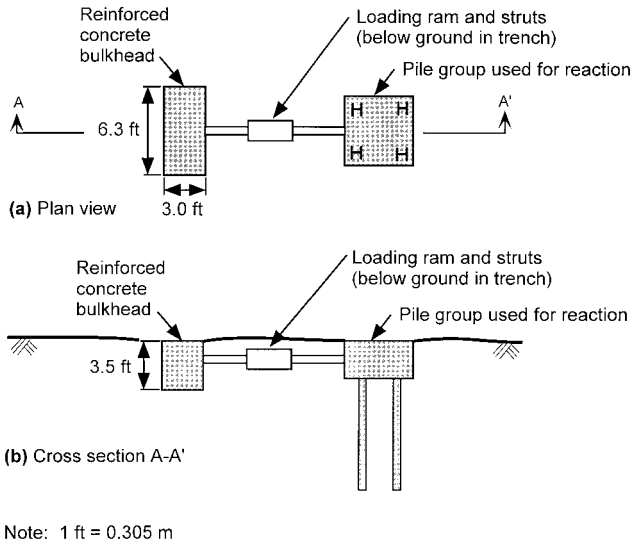

Note: 1 ft = 0.305 m

FIG. 7. Test Arrangement for Passive Pressure Load Tests

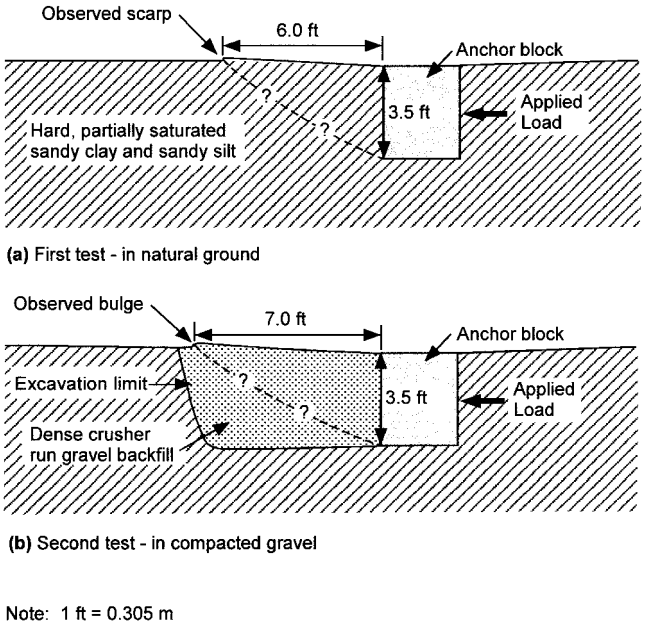

Note: 1 ft = 0.305 m

FIG. 8. Positions of Scarp and Surface Bulge in Passive Pressure Load Tests in Natural Ground and Crusher Run Gravel

other with the anchor block bearing against compacted gravel backfill, as shown in Fig. 8. Both tests were continued to failure, making it possible to measure the ultimate passive resistance and the variation of passive resistance with deflection.

Test Procedures

The anchor block was loaded incrementally. Each load was maintained for about 1 min before applying the next load. The deflection of the anchor block was measured using Celesco cable extension position transducers, and the applied loads were measured using a columnar load cell.

The first test, with the anchor block bearing against natural ground, was performed using load increments ranging from 12.5 to 15 kips (from 56 to 67 kN), up to a maximum load of 138 kips (614 kN). Continual movement occurred when the 138-kip load was applied. After about 90 min, during which the load was maintained while deflections increased to about 1.6 in. (41 mm), the passive resistance dropped off dramatically, indicating failure within the soil in front of the anchor block. Cracks were observed extending outward from the lead corners of the anchor block, in a direction roughly parallel with the direction of loading. The cracks varied in width from hairline to 0.25 in. (6 mm), and the longest was visible for about 3.5 ft (1.1 m) from the anchor block. As shown in Fig. 8(a), a scarp was observed at a distance of about 6.0 ft (1.8 m) from the anchor block and parallel to the front of the anchor block. The anchor block and the passive failure wedge both moved laterally and upward together as the load was increased.

Prior to the second test, the natural soil was excavated from in front of the anchor block to a depth of 3.5 ft (1.1 m) and for a distance of 7.5 ft (2.3 m) from the front of the anchor block, as shown in Fig. 8(b). The excavation extended 1.5 ft (0.5 m) beyond the ends of the anchor block. The excavation was filled with crusher run backfill, compacted in layers. The test was performed using load increments from 10 to 15 kips (from 45 to 67 kN), up to a maximum of 91.7 kips (408 kN), and maximum deflection of about 1.5 in. (38 mm). The surface of the backfill moved upward during the test. As shown in Fig. 8(b), a distinct bulge developed on the surface of the backfill, 7.5 ft (2.3 m) from the front of the anchor block and parallel to the front of the anchor block. Surface cracks extended from the front corners of the anchor block out to the surface bulge. As was the case in the test on the natural soil, the anchor block and the passive failure wedge both moved laterally and upward together as the load was increased.

Soil Properties

The natural soil at the Kentland Farms field test site is desiccated hard sandy silt (ML) and sandy clay (CL). Unconsolidated-undrained triaxial tests were performed on test specimens trimmed from hand-excavated block samples. The results of these tests are shown in Fig. 9(a). Because the undisturbed samples were from above the water table and were only partly saturated, the strength envelope exhibits a large friction angle (32°–38°) as well as a cohesion intercept (1.0 ksf, or 48 kPa). Because the duration of the passive pressure load test was about 1.5 h, a period too short for any significant drainage of this natural soil, these strength parameters are appropriate for use in calculating passive response for comparison with the results of the tests.

Although the block samples and the test specimens were of excellent quality, the results of the tests were somewhat scattered. The ranges of strength parameters and modulus values shown in Tables 5 and 6 are believed to be representative of the in situ behavior of the natural soil.

The gravel backfill used in the second test is crusher run aggregate (GW-GM and SW-SM). Approximately 40–50% of the material passes the No. 4 sieve, 10–20% passes the No. 40 sieve, and 5–10% passes the No. 200 sieve. The gravel was compacted, in layers, to a relative density of about 80%. Drained triaxial tests were performed on specimens that were carefully compacted in the laboratory to the average density measured in the field, using a method developed by Ladd (1978). The tests were conducted at low confining pressures, consistent with the conditions in the field. The results of these tests are shown in Fig. 9(b). The ranges of property values in Tables 5 and 6 are believed to be representative of the behavior of the crusher run gravel, in the condition in which it was compacted in front of the anchor block, at a relative density of about 80%.

The crusher run backfill has high strength and stiffness and would be considered an ideal backfill material. However, in the low range of pressures involved in the passive pressure tests and in the triaxial tests, the natural soil at the site is stronger, because it has a considerable cohesion intercept as well as a sizeable friction angle.

Under long-term conditions, the situation might be reversed.

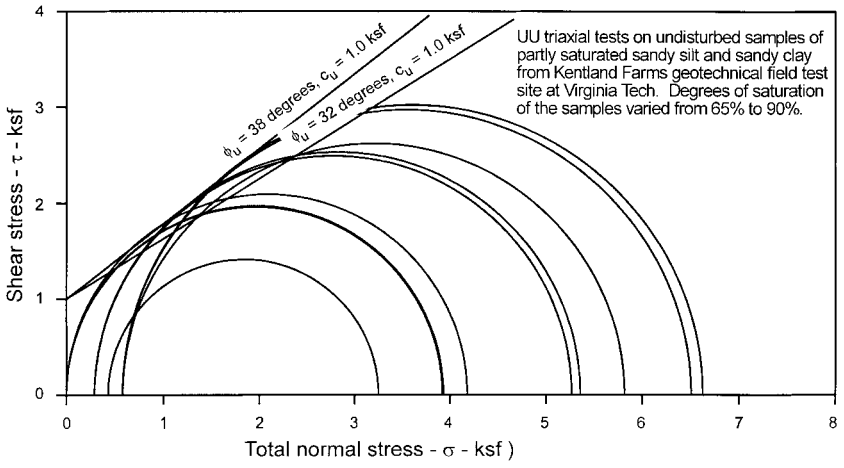

(a) UU triaxial tests on natural soils

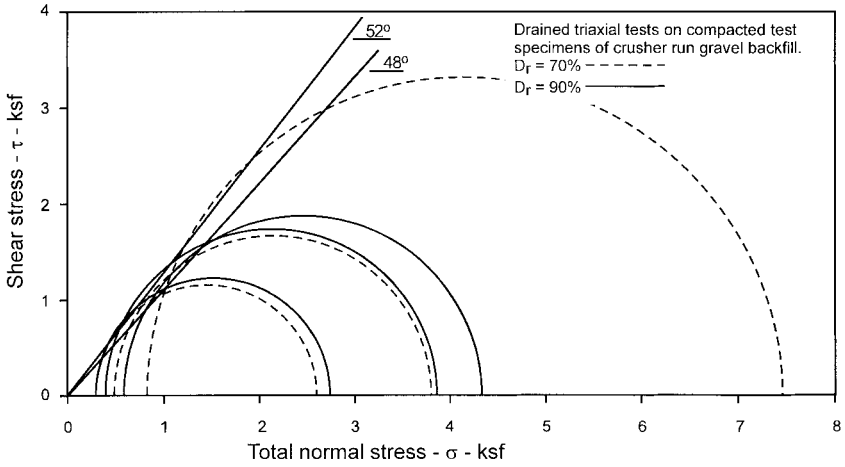

(b) Drained triaxial test on crusher run gravel

Note: 1 ksf = 47.9 kPa

FIG. 9. Strength Envelopes for Naturally Occurring Sandy Silt and Clay, at Kentland Farms Test Site, and Crusher Run Backfill (UU = Unconsolidated-Undrained)

TABLE 5. Measured Shear Strength and Unit Weight of Natural Soil and Crusher Run Gravel Backfill

Soil (1)	Properties (2)
Natural soil	High: c = 1,000 psf, ϕ = 38°, γ = 122 pcf Low: c = 1,000 psf, ϕ = 32°, γ = 135 pcf
Gravel backfill	High: c' = 0, ϕ' = 52°, γ = 135 pcf Low: c' = 0, ϕ' = 48°, γ = 135 pcf

Note: 1 psf = 0.0479 kPa; 1 pcf = 0.157 kN/m^3; c = total stress cohesion intercept, measured in unconsolidated-undrained triaxal tests; ϕ = total stress friction angle, measured in unconsolidated-undrained triaxial tests; c' = total stress cohesion intercept, measured in drained triaxal and direct shear tests; ϕ' = total stress friction angle, measured in drained triaxial and direct shear tests; and γ = total unit weight.

TABLE 6. Elastic Properties of Natural Soil and Crusher Run Gravel Backfill

Soil (1)	Properties (2)
Natural soil	High: E_i = 1,000 ksf (measured in unconsolidated-undrained triaxial tests); ν = 0.33 (estimated) Low: E_i = 700 ksf (measured in unconsolidated-undrained triaxial tests); ν = 0.33 (estimated)
Gravel backfill	High: E_i = 850 ksf (measured in drained triaxial tests); ν = 0.30 (estimated) Low: E_i = 580 ksf (measured in drained triaxial tests); ν = 0.30 (estimated)

Note: 1 ksf = 47.9 kPa; E_i = initial tangent modulus; and ν = Poisson's ratio.

If negative pore pressures in the sandy silt and clay dissipated over time because of rainfall and increase in water content, the strength of the natural soil would decrease. It seems likely that the drained strength of the sandy silt and clay would be smaller than the drained strength of the crusher run gravel shown in Fig. 9(b).

COMPARISON OF MEASURED AND COMPUTED PASSIVE RESISTANCE

Table 7 shows comparisons of the results of the passive pressure load tests with values computed using the three theories discussed previously—Rankine, Coulomb, and Log Spiral, with and without the Ovesen-Brinch Hansen correction for 3D effects. It can be seen that the Log Spiral Theory with the Ovesen-Brinch Hansen correction agrees most closely with the experimental results.

Fig. 10 shows comparisons of measured and computed load-deflection curves, using the log spiral value of P_{ult} corrected for 3D effects. Although there was scatter in the measured values of strength and stiffness of the soils, as indicated in Tables 5 and 6, there is reasonable agreement between the

measured load-deflection behavior and the range of computed values.

There is little difference between the values shown in Table 7 for the Coulomb Theory and the Log Spiral Theory without the Ovesen-Brinch Hansen correction, because the values of interface friction angle are so small. The values of the interface friction angle in these tests were controlled by the weight of the anchor block and the requirements of vertical equilibrium, as shown in Fig. 11. The anchor block, 3.5-ft high by 6.3-ft long by 3.0-ft thick (1.1 × 1.9 × 0.9 m), weighs 9.9 kips (44 kN). Once the vertical component of the passive pressure force reached this magnitude, the anchor block began to move upward with the soil in the passive zone, as that soil slid up along the shear plane.

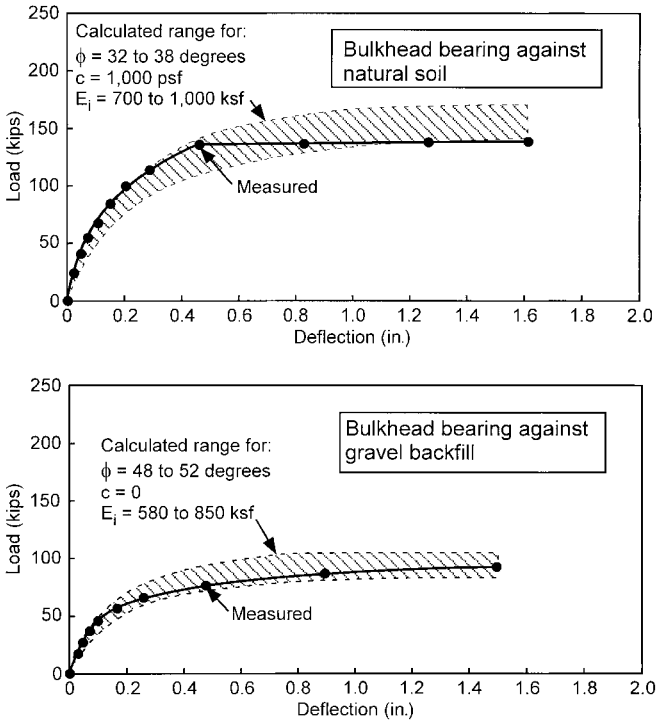

Note: 1 in. = 25.4 mm, 1 kip = 4.45 kN, 1 psf = 0.0479 kPa, 1 ksf = 47.9 kPa

FIG. 10. Computed and Measured Load-Deflection Curves for Passive Pressure Load Tests

TABLE 7. Comparison of Computed and Measured Passive Resistances (kips)

Method (1)	Natural Soil			Gravel Backfill		
	High (2)	Low (3)	Average (4)	High (5)	Low (6)	Average (7)
Rankine	110	94.8	102	43.9	35.4	39.6
Coulomb	119	103	111	59.0	49.4	54.2
Log Spiral, without 3D correction	120	102	111	58.0	48.4	53.3
Log Spiral, with 3D correction	173	139	156	104	82.3	93.2
Measured	—	—	138	—	—	91.7

Note: 1 kip = 4.45 kN; high computed using high strengths in Table 5; and low computed using low strengths in Table 5.

The values of δ_{mob} shown in Fig. 11 were determined by repeated trials. Initially, a value of δ_{mob} was assumed and the corresponding value of E_p was computed. Then the vertical component of E_p was compared to the weight of the anchor block. This process was repeated until the vertical component of E_p was equal to the weight of the anchor block.

On the basis of the results shown in Fig. 10, it appears that the use of the Log Spiral earth pressure theory, together with the Ovesen-Brinch Hansen correction for 3D effects, provides a reasonably accurate means of estimating passive resistance and the variation of passive resistance with deflection, provided suitable values of unit weight, strength, and elastic modulus are used in the calculations.

CONCLUSIONS

Passive resistance to movement of structures is controlled by (1) the amount and direction of movement of the structure, (2) strength and stiffness of the soil, (3) friction and adhesion on the interface between the soil and structure, and (4) shape of the structure.

The Log Spiral passive pressure theory, with the Ovesen-Brinch Hansen correction for 3D (or shape) effects, provides the most accurate theory for computing ultimate passive soil resistance over a wide range of interface friction angles. Elas-

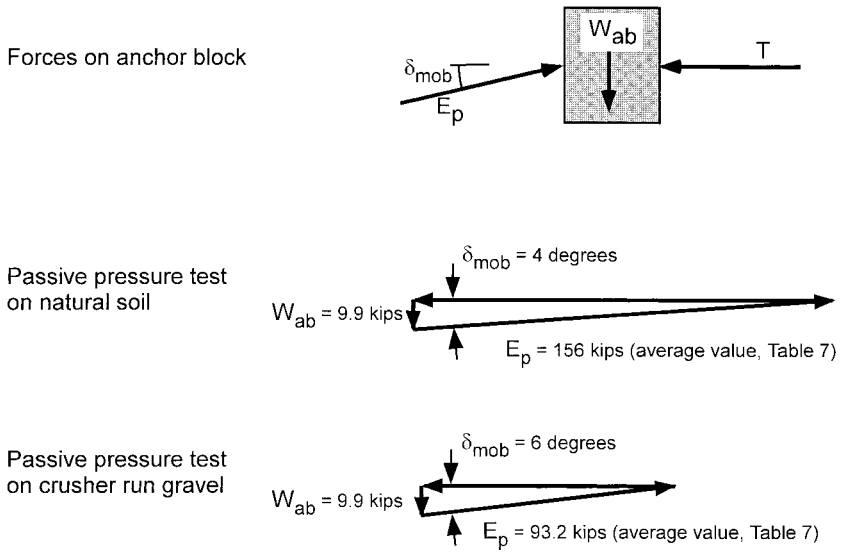

Note: 1 kip = 4.45 kN

FIG. 11. Relationship between W_{ab} and δ_{mob} for Virginia Tech Passive Pressure Tests

tic theory can be used to compute the initial stiffness (the initial slope of the load-deflection curve). The nonlinear variation of passive resistance with deflection can be approximated by a hyperbolic curve that incorporates the initial elastic stiffness and the ultimate passive resistance.

To compute accurate values of passive resistance, it is essential to assess soil strength and stiffness accurately. The shear strength and elasticity parameters used in the calculations must reflect the behavior of the soil in the field, including density, drainage conditions, and range of confining pressure.

ACKNOWLEDGMENTS

The Virginia Transportation Research Council, the Virginia Department of Transportation, Nikken Sekkei, Ltd., and Virginia Tech provided financial support for this study. Sami Arsoy and Brian Metcalf assisted with the laboratory tests and the passive pressure load tests.

APPENDIX. REFERENCES

Brinch Hansen, J. (1966). ''Resistance of a rectangular anchor slab.'' *Bull. No. 21*, Danish Geotechnical Institute, Copenhagen, 12–13.

Caquot, A. I., and Kerisel, J. (1948). ''Tables for the calculation of passive pressure, active pressure, and bearing capacity of foundations.'' *Libraire du Bureau des Longitudes*, de L'ecole Polytechnique, Paris Gauthier-villars, Imprimeur-Editeur, 120.

Chu, S.-C., and Su, J. J. (1994). ''A method for passive pressure earth computation on sands.'' *Proc., 8th Int. Conf. on Methods and Adv. in Geomechanics*, Siriwardane and Zaman, eds., Vol. 3, Balkema, Rotterdam, The Netherlands, 2441–2445.

Coulomb, C. A. (1776). ''Essai sur une application des règles des maximas et minmas à quelques problèmes de statique relatifs à l'architecture.'' *Mém. acad. roy. pres. divers savanta*, Vol. 7, Paris (in French).

Douglas, D. J., and Davis, E. H. (1964). ''The movements of buried footings due to moment and horizontal load and the movement of anchor plates.'' *Géotechnique*, London, 14(2), 115–132.

Duncan, J. M., and Buchignani, A. L. (1976). *An engineering manual for settlement studies*, Dept. of Civ. and Envir. Engrg., Virginia Polytechnic Institute, Blacksburg, Va.

Duncan, J. M., Byrne, P., Wong, K. S., and Mabry, P. (1980). ''Strength, stress-strain and bulk modulus parameters for finite element analysis of stress and movements in soil masses.'' *UCB/GT/80-01*, University of California, Berkeley, Calif.

Duncan, J. M., and Chang, C. Y. (1970). ''Nonlinear analysis of stress and strain in soils.'' *J. Soil Mech. and Found. Div.*, ASCE, 96(5), 1629–1653.

Kumar, J., and Subga Rao, K. S. (1997). ''Passive pressure coefficients, critical failure surface and its kinematic admissability.'' *Géotechnique*, London, 47(1), 185–192.

Ladd, R. S. (1978). ''Preparing test specimens using undercompaction.'' *Geotech. Testing J.*, 1(1), 16–23.

Lambe, T. W., and Whitman, R. V. (1969). *Soil mechanics*, Wiley, New York.

Martin, G. R., and Nad Yan, L. (1995). ''Modelling passive earth pressure for bridge abutments.'' *Earthquake-induced movements and seismic remediation of existing foundations and abutments, Geotech. Spec. Publ. No. 55*, ASCE, New York, 1–16.

Ovesen, N. K. (1964). ''Anchor slabs, calculation methods, and model tests.'' *Bull. No. 16*, Danish Geotechnical Institute, Copenhagen, 5–39.

Potyondy, J. G. (1961). ''Skin friction between various soils and construction materials.'' *Géotechnique*, London, 11(1), 339–353.

Rankine, W. J. M. (1857). ''On the stability of loose earth.'' *Philosophical Trans. Royal Soc.*, London.

Reese, L. C. (1958). ''Discussion of 'Soil modulus for laterally loaded piles,' by B. McIlelland and J. A. Focht.'' *Trans. ASCE*, 123, 1065–1086.

Shields, D. H., and Tolunay, A. Z. (1973). ''Passive pressure coefficients by method of slices.'' *J. Soil Mech. and Found. Div.*, ASCE, 99(12), 1043–1053.

Soubra, A. H. (2000). ''Static and seismic earth pressure coefficients on rigid retaining structures.'' *Can. Geotech. J.*, Ottawa, 37, 463–478.

Terzaghi, K. (1943). *Theoretical soil mechanics*, Wiley, New York.

Terzaghi, K., Peck, R. B., and Mezri, G. (1996). *Soil mechanics in engineering practice*, 3rd Ed., Wiley, New York.

Zhu, D.-Y., and Qian, Q. (2000). ''Determination of passive earth pressure coefficients by the method of triangular slices.'' *Can. Geotech. J.*, Ottawa, 37, 485–491.